JACC: CARDIOONCOLOGY VOL. 2, NO. 5, 2020

ORIGINAL RESEARCH

Dual Angiotensin Receptor-Neprilysin Inhibition With Sacubitril/Valsartan Attenuates Systolic Dysfunction in Experimental Doxorubicin-Induced Cardiotoxicity

Nabil E. Boutagy, PhD,[a] Attila Feher, MD, PhD,[a] Daniel Pfau, BS,[a] Zhao Liu, PhD,[b] Nicole M. Guerrera, AAS, RT(R), RDCS,[a] Lisa A. Freeburg, BA,[c] Sydney J. Womack, BS,[c] Abigail C. Hoenes, BS,[c] Caroline Zeiss, PhD, DACVP, DACLAM,[d] Lawrence H. Young, MD,[a] Francis G. Spinale, MD, PhD,[c] Albert J. Sinusas, MD[a,b]

ABSTRACT

BACKGROUND Doxorubicin (DOX) induces cardiotoxicity in part by activation of matrix metalloproteinases (MMPs). Sacubitril/valsartan (Sac/Val) exerts additive cardioprotective actions over renin-angiotensin-aldosterone inhibitors in preclinical models of myocardial infarction and in heart failure patients. We hypothesized that Sac/Val would be more cardioprotective than Val in a rodent model of progressive DOX-induced cardiotoxicity, and this benefit would be associated with modulation of MMP activation.

OBJECTIVES We sought to investigate the efficacy of Sac/Val for the treatment of anthracycline-induced cardiotoxicity.

METHODS Male Wistar rats received DOX intraperitoneally (15 mg/kg cumulative) or saline over 3 weeks. Following the first treatment, control animals were gavaged daily with water ($n = 25$), while DOX-treated animals were gavaged daily with water ($n = 25$), Val (31 mg/kg; $n = 25$) or Sac/Val (68 mg/kg; $n = 25$) for either 4 or 6 weeks. Echocardiography was performed at baseline, and 4 and 6 weeks after DOX initiation. In addition, myocardial MMP activity was assessed with ^{99m}Tc-RP805, and cardiotoxicity severity was assessed by histology at these time points in a subgroup of animals.

RESULTS Left ventricular ejection fraction decreased by 10% at 6 weeks in DOX and DOX + Val rats (both $p < 0.05$), while this reduction was attenuated in DOX + Sac/Val rats. MMP activity was increased at 6 weeks by 76% in DOX-alone rats, and tended to increase in DOX + Val rats (36%; $p = 0.051$) but was similar in DOX + Sac/Val rats as compared with time-matched control animals. Both therapies attenuated histological evidence of cellular toxicity and fibrosis ($p < 0.05$).

CONCLUSIONS Sac/Val offers greater protection against left ventricular remodeling and dysfunction compared with standard angiotensin receptor blocker therapy in a rodent model of progressive DOX-induced cardiotoxicity. (J Am Coll Cardiol CardioOnc 2020;2:774–87) © 2020 The Authors. Published by Elsevier on behalf of the American College of Cardiology Foundation. This is an open access article under the CC BY-NC-ND license (http://creativecommons.org/licenses/by-nc-nd/4.0/).

From the [a]Section of Cardiovascular Medicine, Department of Medicine, Yale Translational Research Imaging Center, Yale School of Medicine, New Haven, Connecticut, USA; [b]Department of Radiology and Biomedical Imaging, Yale School of Medicine, New Haven, Connecticut, USA; [c]Department of Cell Biology & Anatomy, University of South Carolina School of Medicine, Columbia, South Carolina, USA; and the [d]Section of Comparative Medicine, Yale School of Medicine, New Haven, Connecticut, USA.

ISSN 2666-0873 https://doi.org/10.1016/j.jaccao.2020.09.007

Cancer-related mortality has significantly declined over the past 30 years due to more effective education, screening, and treatment options. However, the use of a common chemotherapeutic class, anthracyclines, can result in anthracycline-induced cardiotoxicity (AIC) (1). For example, doxorubicin (DOX) (Adriamycin), the most widely used anthracycline, is associated with AIC in up to 26% of patients and can progress to severe left ventricular (LV) failure (1). This form of AIC is generally thought to be irreversible, as 45% of chemotherapy patients who develop LV failure do not improve with standard-of-care medical therapy (2). Although there are likely multiple pathways that contribute to AIC, one downstream pathway that causes LV myocardial remodeling and failure are shifts in proteolytic pathways such as the matrix metalloproteinases (MMPs) and tissue inhibitors of metalloproteinases (TIMPs). Our group and others have shown that the steady-state balance of myocardial MMP is disrupted in animal models of AIC (3,4). Furthermore, we demonstrated that the severity of LV dysfunction is associated with the magnitude of MMP activity following DOX administration, assessed by ^{99m}Tc-RP805, a radiolabeled tracer that binds (at nanomolar concentrations) to the active catalytic site of several MMPs (MMP-2, MMP-3, MMP-7, MMP-9, MMP-12, and MMP-13) but not to other proteolytic enzymes (5,6). We have also demonstrated that ^{99m}Tc-RP805 myocardial uptake strongly correlates to ex vivo MMP activity (5,7). Notably, several MMP isoforms that ^{99m}Tc-RP805 detects have been shown to be upregulated in the myocardium of various animal models of AIC (8,9) and in the circulation of patients treated with DOX (10). Thus, it stands to reason that pharmacotherapies that modify MMP activity may hold relevance in the context of AIC, and that ^{99m}Tc-RP805 can be used to assess changes in MMP-TIMP balance.

Prior animal studies have shown that activation of the renin-angiotensin-aldosterone system (RAAS) can contribute to the development and progression of AIC (11), whereas RAAS inhibition with either angiotensin-converting enzyme inhibitors or angiotensin receptor antagonists reduces the degree of adverse cardiac remodeling associated with AIC (12,13). Along these lines, some small human studies have shown a potential benefit of RAAS inhibitors in attenuating the development and degree of AIC (14,15); however, other studies fail to report benefit (16,17). Together, these findings suggest that signaling pathways over and above that of RAAS signaling exist in the pathogenesis of AIC.

Sacubitril/valsartan (Sac/Val) is a first-in-class clinically available angiotensin receptor-neprilysin inhibitor that reduced cardiovascular events in patients with heart failure (18). Neprilysin is a neutral endopeptidase that can modify a number of biological signaling pathways that may hold relevance in the context of AIC. Prior studies have shown that Sac/Val can provide additional protective effects compared with RAAS inhibition alone, mainly in rodent models of myocardial infarction (19,20). In some of these studies, evidence was provided that Sac/Val favorably shifted myocardial MMP-TIMP balance (20). In an initial study, Sac/Val reduced myocardial injury and improved LV function following a high dose of DOX (21). Based on these past findings, this study used a clinically relevant rodent model to test the hypothesis that Sac/Val would be more protective against AIC than Val in part due to modulation of MMP activation.

ABBREVIATIONS AND ACRONYMS

AIC = anthracycline-induced cardiotoxicity

ARB = angiotensin receptor blocker

DOX = doxorubicin

LV = left ventricular

LVEF = left ventricular ejection fraction

MMP = matrix metalloproteinase

RAAS = renin-angiotensin-aldosterone system

SAC = sacubitril

TIMP = tissue inhibitor of metalloproteinases

Val = valsartan

METHODS

ANIMAL MODEL. A schematic of the overall study design is illustrated in **Figure 1**. Male Wistar rats (10 to 11 weeks old) were purchased from Charles River Laboratories (Wilmington, Massachusetts) and were acclimatized to their environment for 5 days before any study procedures. All animals were housed in a temperature-controlled facility (22°C to 24°C), kept on a 12-h light/dark cycle, and fed a standard chow diet ad libitum for the duration of the study. All animals were used in accordance with protocols and policies approved by the Yale Institutional Animal Care and Use Committee and in accordance with all provisions of the Public Health Service Policy on Humane Care and Use of Laboratory Animals (National Institutes of Health assurance: D16-00146 [A3230-01]).

The authors attest they are in compliance with human studies committees and animal welfare regulations of the authors' institutions and Food and Drug Administration guidelines, including patient consent where appropriate. For more information, visit the Author Center.

Manuscript received June 19, 2020; revised manuscript received September 8, 2020, accepted September 9, 2020.

FIGURE 1 Schematic of Experimental Design

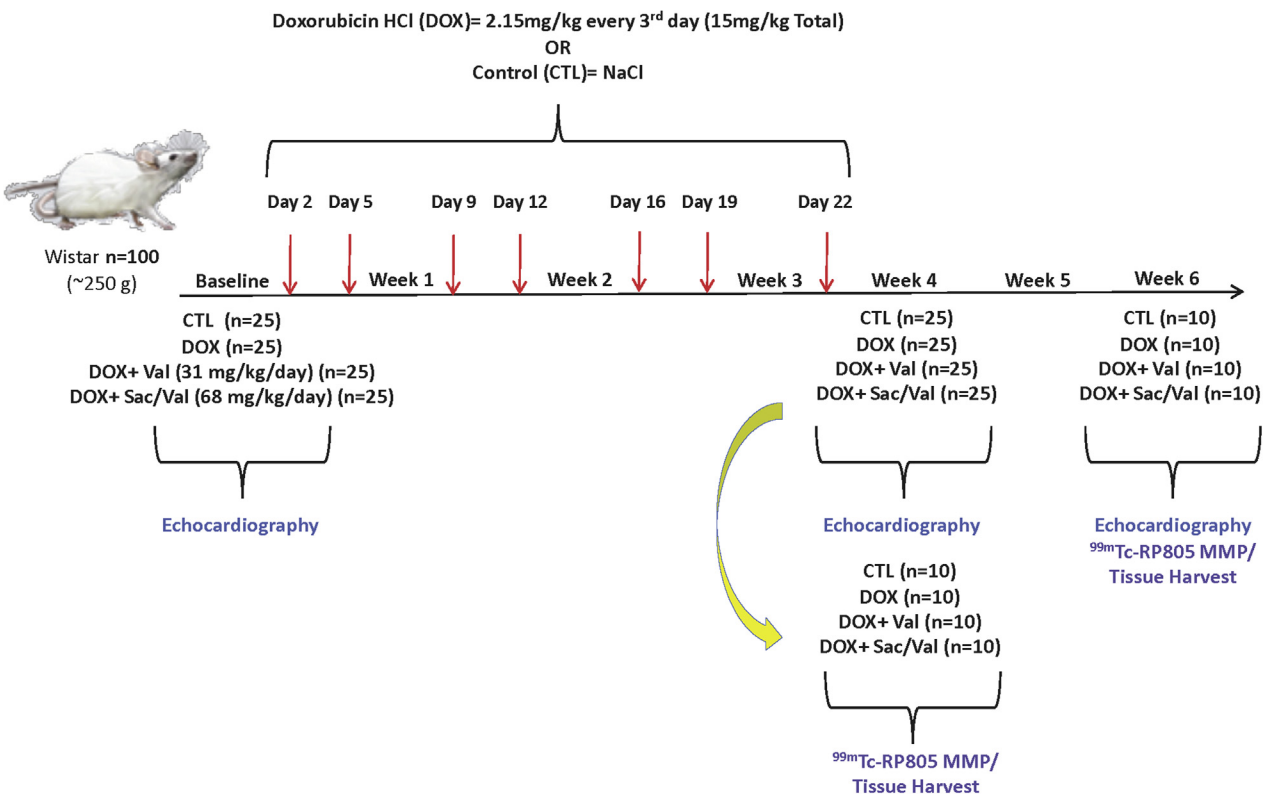

A parallel group design was employed for 6 weeks using 4 groups of rats (n = 25 each group; N = 100). The groups included control (CTL) animals, doxorubicin (DOX)-treated rats (DOX), DOX-treated rats receiving valsartan (Val) (DOX + Val), and DOX-treated rats receiving sacubitril (Sac)/Val (DOX + Sac/Val). Animals were treated with either DOX (2.15 mg/kg/dose, 15 mg/kg total, n = 75) or saline (CTL group, n = 25) every 3 days for 21 days, denoted by **red arrows**. Following the first treatment, CTL animals were gavaged daily with water (n = 25), while DOX-treated animals were gavaged daily with water (n = 25), Val (31 mg/kg; n = 25), or Sac/Val (68 mg/kg; n = 25) for 4 to 6 weeks. Echocardiography was performed at baseline (prior to chemotherapy, n = 25 per group) and at 4 weeks (n = 25 per group) and 6 weeks (n = 10 per group) following initiation of chemotherapy to assess changes in cardiac function. In a subgroup of rats, myocardial matrix metalloproteinase (MMP) activity and cardiotoxicity severity were assessed ex vivo with ^{99m}Tc-RP805 and standard histological techniques (n = 7 to 10 per group), respectively, at 4 and 6 weeks following the first chemotherapy dose.

This study employed an established model of chronic progressive cardiotoxicity as previously described (3). Specifically, rats were either intraperitoneally administered DOX (2.15 mg/kg) every 3 days for 21 days (15 mg/kg total) (n = 75) or an equal volume of 0.9% saline (control group, n = 25) in an identical fashion. Following the first dose of DOX, animals in the DOX groups either remained untreated (DOX group, n = 25), or were administered Val (31 mg/kg in water [pH 8.0]) (DOX + Val group, n = 25) or Sac/Val (68 mg; 1/1 ratio of Sac [31 mg] and Val [31 mg Val] in water with 6 mg of sodium [pH 8.0]) (DOX + Sac/Val group, n = 25) daily by gavage for the duration of study. This dose of Sac/Val was chosen based on prior preclinical studies defining the pharmacokinetics and pharmacodynamics of Sac/Val in rats (22) and other studies demonstrating beneficial effects of Sac/Val on myocardial remodeling in rats (20). To control for any potential influence of oral gavaging, both the control and the DOX-alone groups received daily oral administrations of water in an identical fashion to the treated groups.

EXPERIMENTAL DESIGN. Systolic function and LV dimensions were measured with 2-dimensional echocardiography in all animals at baseline (n = 100). Four weeks following the first chemotherapy dose, cardiac function was reassessed by echocardiography (n = 100). At this time, a subgroup of animals (n = 10 per group) were injected with ^{99m}Tc-RP805, a radiotracer that binds to the catalytic site of activated MMPs (5), for quantitative assessment of myocardial ^{99m}Tc-RP805 uptake with gamma well counting. In addition, LV tissue was harvested to assess the degree of cardiotoxicity with standard histopathologic techniques.

At 6 weeks following the initiation of DOX, the remaining animals in each group (n = 8 to 10 per group) had cardiac function reassessed with 2-dimensional echocardiography along with LV MMP activity and the degree of cardiotoxicity, as described previously (3). We experienced approximately a 20% mortality across all groups due to experimental handling and systemic DOX toxicity. See the Supplemental Appendix for detailed methods.

STATISTICAL ANALYSIS. Statistical analyses were performed with Prism 8 (GraphPad Software, San Diego, California) and SPSS version 26 (IBM, Armonk, New York). All data were tested for normality with a Shapiro-Wilk normality test. For repeated-measures analysis, echocardiography data were analyzed by fitting a mixed model. This mixed model uses a compound symmetry covariance matrix and is fit using restricted maximum likelihood. To account for variance in baseline, only significant changes from baseline are reported for volumetric measurements. Analysis of variance was used for other comparisons among groups. Post hoc pairwise comparisons were performed using Tukey's multiple comparison test. Pearson's product-moment correlation coefficients (r) were used to determine relationships between continuous variables of interest. Test-retest reliability of echocardiographic measurements was evaluated by calculating the intraclass correlation coefficient from 2 separate measurements of each echocardiographic parameter from 25 animals at baseline. All data are expressed as mean ± SEM. The significance level was set a priori at $p < 0.05$.

RESULTS

TRANSTHORACIC ECHOCARDIOGRAPHY-DERIVED SYSTOLIC FUNCTION AND LV DIMENSIONS. The test-retest reliability for the echocardiographic measurements was excellent (intraclass correlation coefficient >0.96) (Supplemental Table 1). Six weeks after chemotherapy initiation, LV ejection fraction (LVEF) was significantly reduced in DOX rats compared with baseline (77.90 ± 1.20% vs. 69.70 ± 2.30%; $p < 0.05$) and age- and time-matched control animals (77.30 ± 1.80% vs. 69.70 ± 2.30%; $p < 0.05$) (**Figure 2A**). Val treatment in DOX animals (DOX + Val) did not attenuate the reduction in LVEF compared with baseline (79.90 ± 0.63% vs. 69.50 ± 1.80%; $p < 0.05$) or age- and time-matched control animals (77.30 ± 1.80% vs. 69.50 ± 1.80%; $p < 0.05$) at this time point. Conversely, Sac/Val treatment in DOX animals (DOX + Sac/Val) attenuated the DOX-induced reduction in LVEF at 6 weeks. Specifically, LVEF was not significantly different from baseline (77.50 ± 0.97% vs. 74.60 ± 1.70%; $p > 0.05$) or compared with age- and time-matched control animals (77.3 ± 1.80% vs. 74.60 ± 1.70%; $p > 0.05$) at this time point. Fractional shortening was used as an independent index of systolic function and was also reduced after 6 weeks in DOX-treated rats (**Figure 2B**). Similarly, treatment of DOX rats with Val was unable to prevent this decline, whereas treatment with Sac/Val was effective at preserving fractional shortening (**Figure 2B**).

In control animals, LV end-diastolic volume significantly increased from baseline (267.30 ± 0.21 μl) at 4 weeks (327.50 ± 0.25 μl; $p < 0.0001$) and at 6 weeks (325.90 ± 0.58 μl; $p < 0.01$). DOX treatment blunted this growth associated increase in LV end-diastolic volumes from baseline (244.80 ± 0.21 μl) at 4 weeks (273.10 ± 0.25 μl; $p < 0.05$) and at 6 weeks (265.60 ± 0.68 μl; $p > 0.05$) (**Figure 2C**). Neither Val nor Sac/Val prevented this DOX-induced delay in LV end-diastolic volume increases over time. Aligned with changes in systolic function, a time-dependent increase in LV end-systolic volume from baseline was evident at 6 weeks following initiation of chemotherapy in only DOX rats (79.80 ± 0.45 μl vs. 55.20 ± 0.17 μl; $p < 0.05$) and DOX + Val rats (86.30 ± 0.39 μl vs. 49.50 ± 0.13 μl; $p < 0.05$). There was no change in LV end-systolic volume from baseline in DOX rats treated with Sac/Val (72.20 ± 0.38 μl vs. 57.60 ± 0.16 μl; $p > 0.05$) (**Figure 2D**).

TEMPORAL CHANGES IN MYOCARDIAL ^{99m}Tc-RP805 ACTIVITY. LV ^{99m}Tc-RP805 uptake increased significantly in DOX rats (0.030 ± 0.004% ID/g) compared with time-matched control animals (0.017 ± 0.001% ID/g) at 6 weeks ($p < 0.05$) (**Figure 3A**). Similarly, ^{99m}Tc-RP805 uptake trended to increase in DOX + Val rats (0.027 ± 0.003% ID/g) compared with time-matched control animals at 6 weeks ($p = 0.051$). Sac/Val treatment prevented the DOX-induced elevation in MMP activity, as evidenced by ^{99m}Tc-RP805 uptake values being not significantly different from control animals (0.019 ± 0.002% ID/g; $p > 0.05$) (**Figure 3A**). In addition, we observed a significant inverse linear correlation between ^{99m}Tc-RP805 uptake and LVEF ($r = -0.60$; $p = 0.001$) at 6 weeks following chemotherapy initiation (**Figure 3B**). Similarly, ^{99m}Tc-RP805 uptake was modestly correlated to LV end-systolic volume at this time point ($r = 0.49$; $p = 0.003$) (**Figure 3C**).

HISTOPATHOLOGY. **Figure 4** shows representative histological images for each of the groups at 4 and 6 weeks following initiation of chemotherapy. As expected, DOX-treated animals exhibited the most severe intercellular edema, which was evident by 4 weeks and markedly progressed over time. These

FIGURE 2 Transthoracic Echocardiography–Derived Systolic Function and Ventricular Dimensions

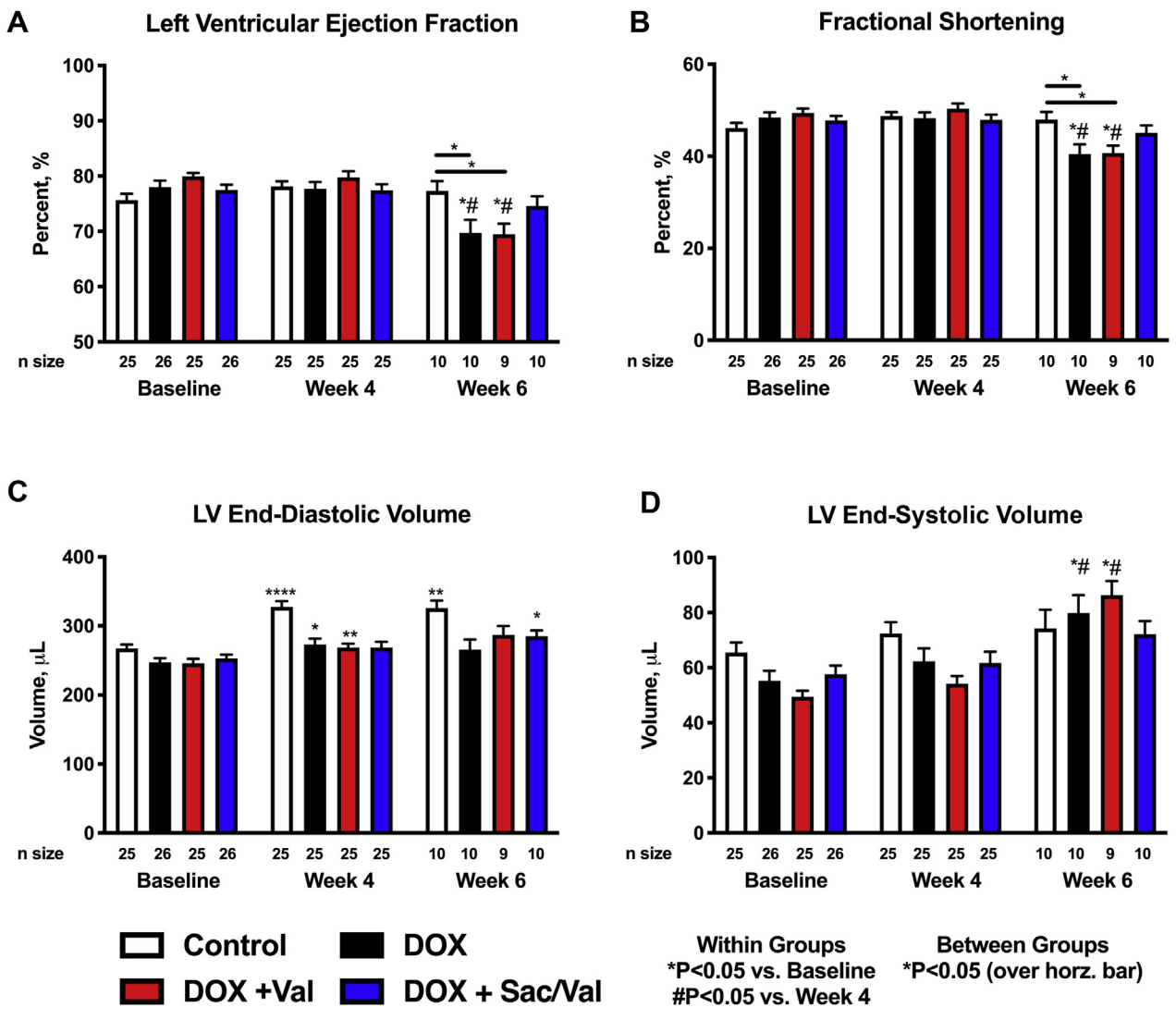

(A) Left ventricular (LV) ejection fraction, **(B)** fractional shortening, **(C)** LV end-diastolic volume, and **(D)** LV end-systolic volume at baseline (n = 25 per group), 4 weeks (n = 25 per group), and 6 weeks (CTL, n = 10; DOX, n = 10; DOX + Val, n = 9, DOX + Sac/Val, n = 10) following the initiation of chemotherapy. *p < 0.05 over horizontal bars indicates between-group difference. *p < 0.05 vs. baseline; **p < 0.01 vs. baseline; ****p < 0.0001 vs. baseline; #p < 0.05 vs. 4 weeks. Abbreviations as in Figure 1.

changes were accompanied by marked variation in myofiber diameter (blue arrows in Figures 4B, 4F, 4J, and 4N) and intracellular vacuolation characteristic of AIC (black arrows in Figures 4F and 4N). As shown in Figure 5, these qualitative changes are supported by semi-quantitative scoring (see Table 1). Specifically, variation in myofiber diameter and intracellular vacuolation was significantly increased in DOX animals compared with control animals at 6 weeks (0.50 ± 0.16 arbitrary units vs. 1.50 ± 0.29 arbitrary units; p < 0.01) (Figure 5A). In addition, inflammatory cell infiltration associated with myofiber variation or vacuolation was also significantly increased in DOX animals at 6 weeks compared with age- and time-matched control animals (0.20 ± 0.13 arbitrary units vs. 0.40 ± 0.16 arbitrary units; p < 0.05) (Figure 5B). Notably, treatment of DOX animals with either Val or Sac/Val resulted in a significant attenuation of DOX-induced changes in myofiber variation or vacuolation (Val: 0.40 ± 0.16 arbitrary units; Sac/Val: 0.33 ± 0.17 arbitrary units) and cellularity (Val: 0.80 ± 0.2 arbitrary units; Sac/Val: 0.78 ± 0.92 arbitrary units at 6 weeks) (Figures 5A and 5B); however, small foci of inflammatory cells (white arrows in Figures 4G, 4H,

FIGURE 3 LV ^{99m}Tc-RP805 Uptake

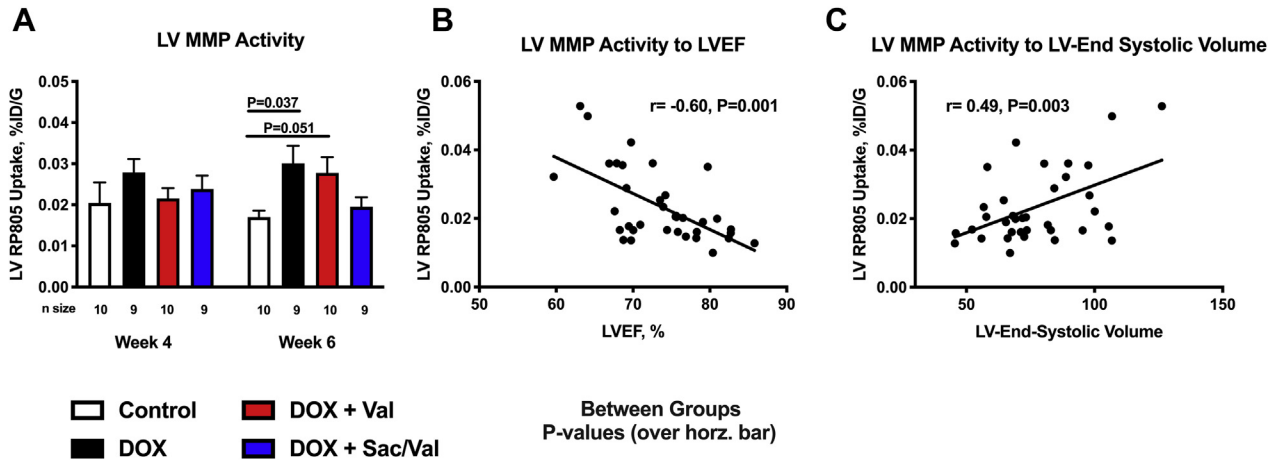

(A) LV ^{99m}Tc-RP805 uptake between CTL animals (n = 10) and rats treated with DOX (n = 9), DOX + Val (n = 10), and DOX + Sac/Val (n = 9) at 4 weeks and between CTL animals (n = 10) and rats treated with DOX (n = 9), DOX + Val (n = 10), and DOX + Sac/Val (n = 9) at 6 weeks following chemotherapy initiation. Correlation between **(B)** LV ejection fraction and LV ^{99m}Tc-RP805 uptake and **(C)** LV end-systolic volume and LV ^{99m}Tc-RP805 uptake in all rats at 6 weeks. *p < 0.05 between group difference. Abbreviations as in Figures 1 and 2.

and 4L) or rare vacuolated myofibers (black arrow in Figure 4P) are still seen.

Because cardiac fibrosis is often observed in humans on biopsy and imaging following DOX administration (23), we chose to assess fibrosis with more quantitative methods. Representative images for Picrosirius red staining and α-smooth muscle actin immunohistochemistry are shown in Figures 6A and 6B for each group at both time points. As shown quantitatively in Figure 6C, there was a significant early increase in the percent of Picrosirius red area in DOX-alone rats compared with time-matched control animals at 4 weeks (4.19 ± 0.23% vs. 2.26 ± 0.16%; p < 0.0001). This increase in collagen content was significantly attenuated in both the DOX + Val (2.91 ± 0.23%; p < 0.01) and DOX + Sac/Val (2.68 ± 0.12%; p < 0.001) rats compared with DOX-alone rats (4.19 ± 0.23%) (Figure 6C). At 6 weeks, collagen content remained elevated in DOX-alone rats compared with time-matched control animals (4.63 ± 0.23% vs. 2.76 ± 0.29%; p < 0.0001). In addition, collagen content significantly increased from 4 to 6 weeks in DOX + Val (2.91 ± 0.23% vs. 3.95 ± 0.20%; p < 0.05) and DOX + Sac/Val rats (2.68 ± 0.12% vs. 3.87 ± 0.26%; p < 0.05), leading to significantly elevated collagen content compared with time-matched control animals at 6 weeks (both p < 0.01) (Figure 6C). α-smooth muscle actin, a marker of myofibroblast expression, showed similar temporal changes to those observed in collagen content (Figures 6B to 6D). Specifically, α-smooth muscle actin expression was significantly elevated at 4 weeks in all DOX-treated animals (DOX: 7.33 ± 0.50%; DOX + Val: 4.88 ± 0.29%; DOX + Sac/Val: 4.93 ± 0.40%) compared with control animals (2.36 ± 0.15%) (all p < 0.0001). However, this elevation was significantly less in DOX + Val and DOX + Sac/Val rats compared with DOX-alone rats (both p < 0.0001). At 6 weeks, α-smooth muscle actin levels remained elevated in DOX-treated rats compared to control animals (7.68 ± 0.41% vs. 3.64 ± 0.23%; p < 0.0001). α-smooth muscle levels were also higher in DOX + Val (4.99 ± 0.20%) and DOX + Sac/Val (4.84 ± 0.33%) rats compared to control animals (both p < 0.05), although these levels were significantly lower than observed in DOX-alone rats (both p < 0.0001) (Figures 6B to 6D).

CAPILLARY DENSITY AND MYOCYTE CROSS-SECTIONAL AREA. Representative fluorescent images of myocyte cross-sectional area and capillary density are shown in Figure 7 for each group at 4 and 6 weeks following initiation of chemotherapy. Myocyte cross-sectional area was reduced in all DOX-treated groups (DOX: 358.3 ± 15.4 μm^2; DOX + Val: 341.6 ± 9.2 μm^2; p < 0.05; DOX + Sac/Val: 310.5 ± 12.5 μm^2; p < 0.05) when compared with time-matched control animals (393.5 ± 16.7 μm^2) at 4 weeks, although this reduction did not reach statistical significance in the DOX-alone group (p > 0.05) (Figures 7A and 7B). Similarly, at 6 weeks, myocyte cross-sectional area was significantly reduced in all DOX-treated groups (DOX: 344.9 ± 10.9 μm^2; DOX + Val: 315.9 ± 10.0 μm^2; DOX + Sac/Val: 327.3 ± 12.8 μm^2) compared with time-matched control

FIGURE 4 Representative Pathohistological Images Over Time

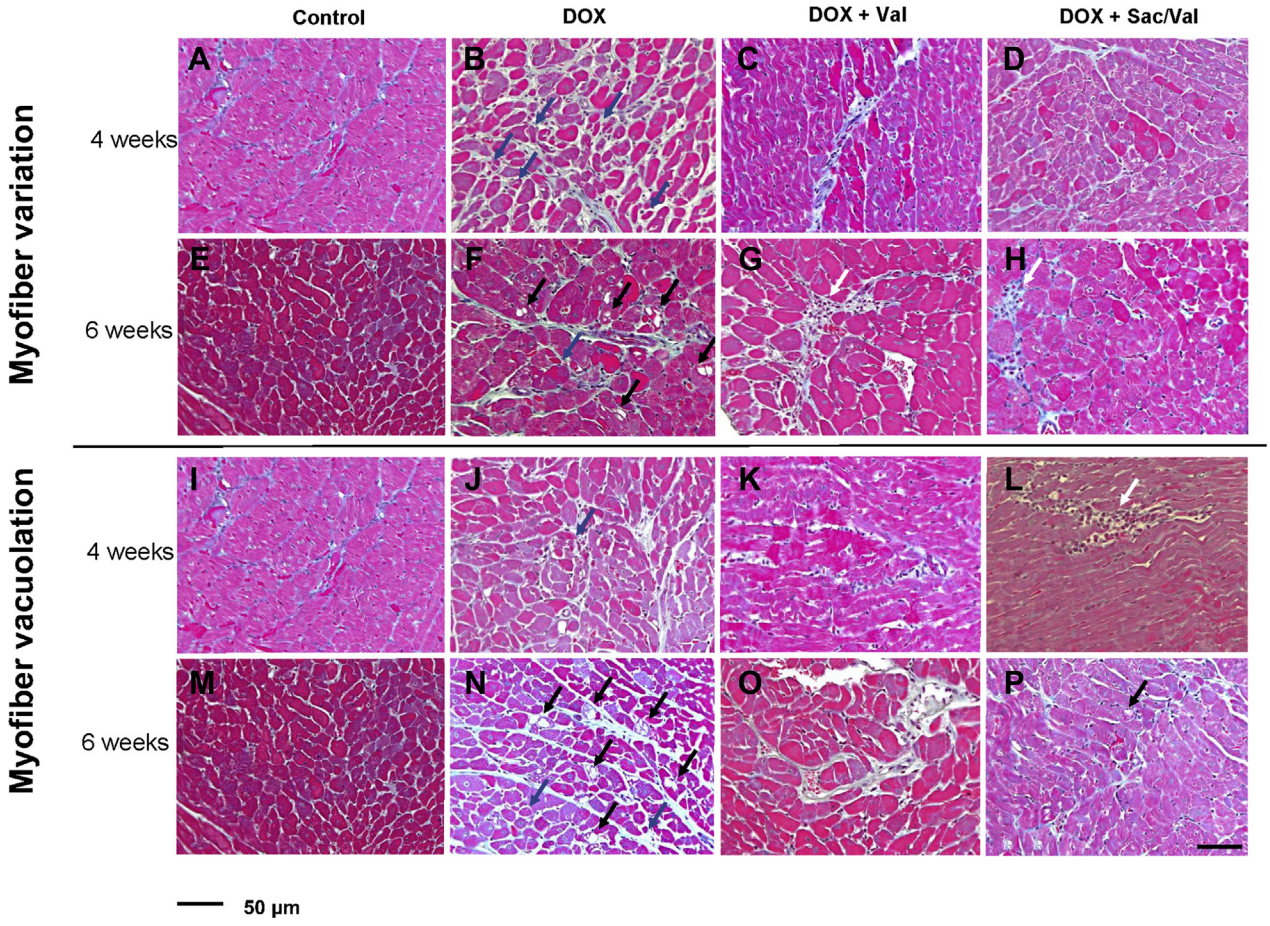

Representative images (Hematoxylin and Eosin [H and E] and Masson's Trichrome [MT]) of myofiber variation **(top panel)** and myofiber vacuolation with cellularity **(bottom panel)** for each group at 4 and 6 weeks following initiation of chemotherapy. Doxorubicin toxicity was progressive and characterized by marked variation in myofiber diameter **(blue arrows, B, F, J, N)** and intracellular vacuolation **(black arrows, F and N)**. Small foci of inflammatory cells **(white arrows, G, H, I)** or rare vacuolated myofibers **(black arrow, P)** are still seen in DOX rats treated with Val and Sac/Val, albeit less than that observed without these treatments. Abbreviations as in Figures 1 and 2.

animals ($437.0 \pm 9.9\ \mu m^2$ vs. $7.3 \pm 12.8\ \mu m^2$; all $p < 0.05$) (Figures 7A and 7B). In line with these findings, total heart weight measured at the time of euthanasia was significantly less in all DOX-treated animals at both 4 and 6 weeks following chemotherapy initiation, regardless of therapy (Supplemental Figure 1C).

At 4 weeks, capillary density was not different between the DOX-alone group (1.15 ± 0.04) and control animals (0.93 ± 0.04) (Figures 7A and 7C). However, treatment of DOX rats with either Val (1.31 ± 0.11; $p < 0.01$) or Sac/Val (1.54 ± 0.06; $p < 0.001$) led to a significant increase in capillary density compared with control animals. The increase in capillary density was also significantly higher in the DOX + Sac/Val rats compared with DOX rats ($p < 0.01$) at this time point. At 6 weeks, capillary density was significantly higher in the DOX (1.34 ± 0.10) and DOX + Val (1.35 ± 0.10) groups compared with time-matched control animals (0.85 ± 0.04) (both $p < 0.001$). On the other hand, capillary density was significantly reduced from 4 to 6 weeks in the DOX + Sac/Val group (1.54 ± 0.06 vs. 1.10 ± 0.08; $p < 0.01$) to levels that were no different from control values at this later time point.

CELLULAR DEATH. Representative fluorescent images for DAPI and TUNEL are shown in Supplemental Figure 1 for each group at 4 and 6 weeks following initiation of chemotherapy. Unlike the observed progressive histopathological changes described previously, cellular apoptosis was not

FIGURE 5 Quantification of Histopathology Scoring Over Time

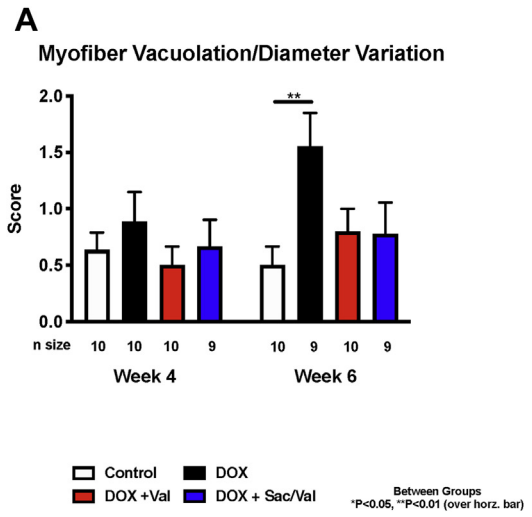

Scoring was categorized as **(A)** myofiber vacuolation with diameter variation and **(B)** cellularity between CTL animals (n = 10) and rats treated with DOX (n = 10), DOX + Val (n = 10), and DOX + Sac/Val (n = 9) at 4 weeks and between CTL animals (n = 10) and rats treated with DOX (n = 9), DOX + Val (n = 10) and DOX + Sac/Val (n = 9) at 6 weeks following chemotherapy initiation. *p < 0.05, **p < 0.01 over horizontal over horizonal bars denotes between-group difference. Abbreviations as in Figure 1.

FIGURE 6 Representative PSR and SMA Staining Images and Quantification

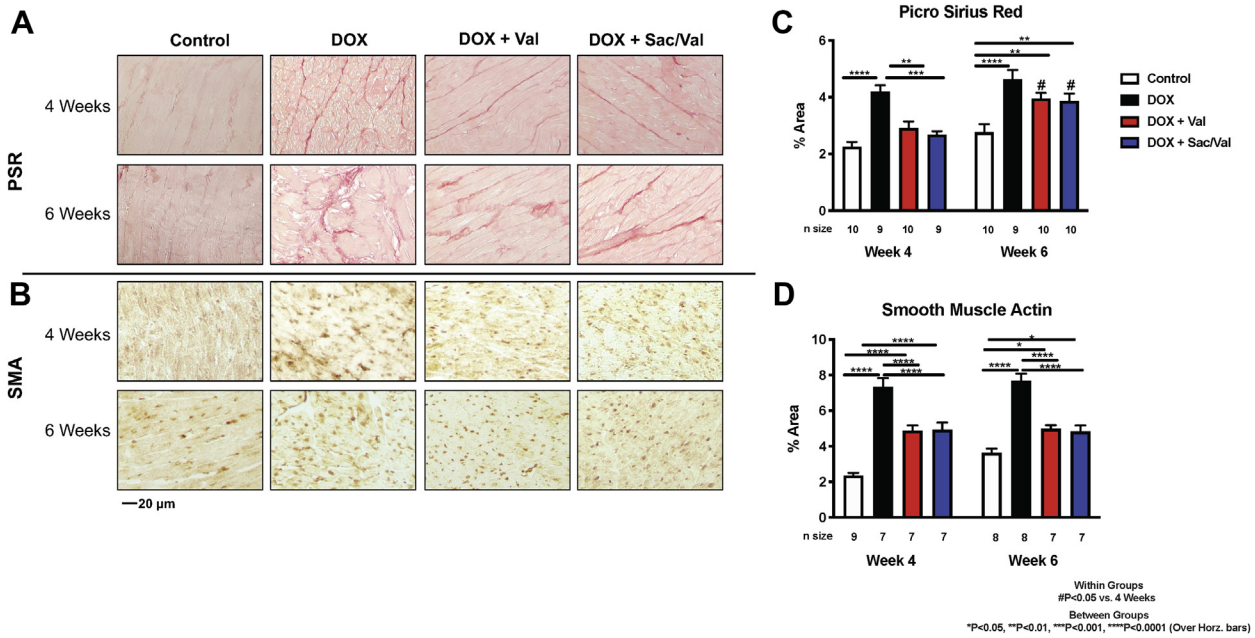

(A) Picrosirius red (PSR) and **(B)** smooth muscle actin (SMA) staining and **(C, D)** respective quantification of these variables between CTL animals (n = 9) and rats treated with DOX (n = 7), DOX + Val (n = 7) and DOX + Sac/Val (n = 7) at 4 weeks and between CTL animals (n = 8) and rats treated with DOX (n = 8), DOX + Val (n = 7) and DOX + Sac/Val (n = 7) at 6 weeks following chemotherapy initiation. * p < 0.05, **p < 0.01, ***p < 0.001, ****p < 0.0001 over horizontal bars denotes between-group difference. #p < 0.05 vs. 4 weeks. Abbreviations as in Figure 1.

FIGURE 7 Cardiomyocyte Cross-Sectional Area and Capillary Density Over Time

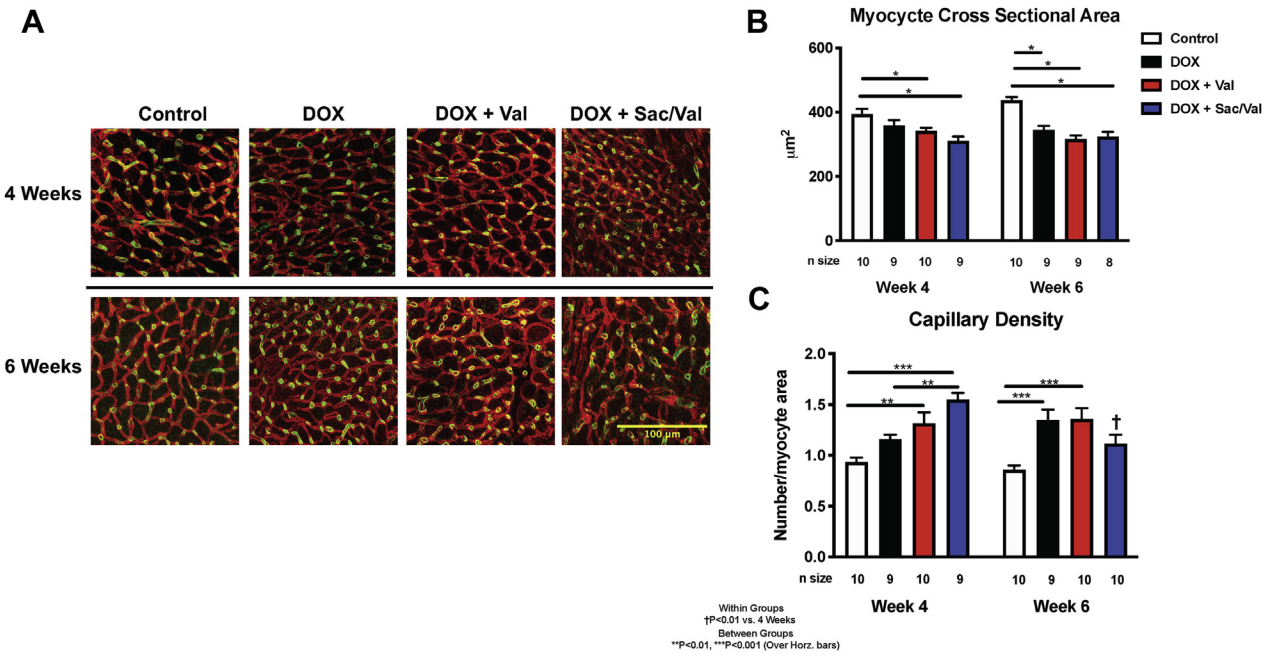

(A) Representative images of LV sections co-stained with laminin **(red)** and isolectin B4 **(green)** at 4 and 6 weeks after the initiation of chemotherapy. **(B)** Quantification of myocyte cross-sectional area (μm^2) and **(C)** capillary density (expressed as capillary number per cardiomyocyte area) for CTL animals (n = 10) and rats treated with DOX (n = 9), DOX + Val (n = 10), and DOX + Sac/Val (n = 9) at 4 weeks and for CTL animals (n = 10) and rats treated with DOX (n = 9), DOX + Val (n = 9–10), and DOX + Sac/Val (n = 8–10) at 6 weeks following chemotherapy initiation. **Horizontal bars** denote group difference at the significance levels of, *p < 0.05, **p < 0.01, and ***p < 0.001. †p < 0.01 vs. 4 weeks. Abbreviations as in Figures 1 and 2.

significantly different among the groups at either time point following the initiation of chemotherapy (Supplemental Figures 1A and 1B).

DISCUSSION

The major finding from the present study is that Sac/Val, a first-in-class clinically approved angiotensin receptor-neprilysin inhibitor, resulted in preserved LV systolic function in an established rodent model of progressive AIC. Conversely, standard angiotensin receptor blocker (ARB) therapy with Val was insufficient to preserve LVEF following DOX administration in this model. In addition, only Sac/Val therapy was able to attenuate the late DOX-induced elevations in LV myocardial ^{99m}Tc-RP805 uptake, a sensitive index of myocardial MMP activity. A possible compensatory increase in capillary density was seen in DOX rats treated with either Val or Sac/Val at the early time point that was more pronounced in the Sac/Val-treated rats. Interestingly, DOX rats treated with either Val or Sac/Val showed a reduction in histological evidence of myocardial toxicity and fibrosis, suggesting that the preservation of LVEF with Sac/Val is due, at least in part, to altered extracellular matrix remodeling secondary to a reduction in myocardial MMP activity (**Central Illustration**).

The precise cellular and molecular mechanisms of AIC are not fully elucidated, although the prevailing hypothesis is that DOX alters redox balance through multiple pathways (24). Consequently, these events culminate into structural remodeling and cardiac dysfunction (24). Thus, therapeutic strategies to prevent or attenuate DOX-induced cardiotoxicity have focused on direct targeting of reactive oxygen species or inhibition of key pathways in the remodeling process. Several preclinical studies report that RAAS inhibition with both angiotensin-converting enzyme inhibitors and ARBs during anthracycline therapy reduce oxidative stress and histological evidence of cardiotoxicity (14,25). In addition, some (15) but not all (17,26) clinical trials report an attenuation in AIC with these therapies. Although these mixed results can be partially explained by trial design, they highlight that novel pharmacotherapies that target pathways other than RAAS are needed. Along these

CENTRAL ILLUSTRATION **Sac/Val Is Superior to Val at Reducing Anthracycline-Induced Cardiotoxicity**

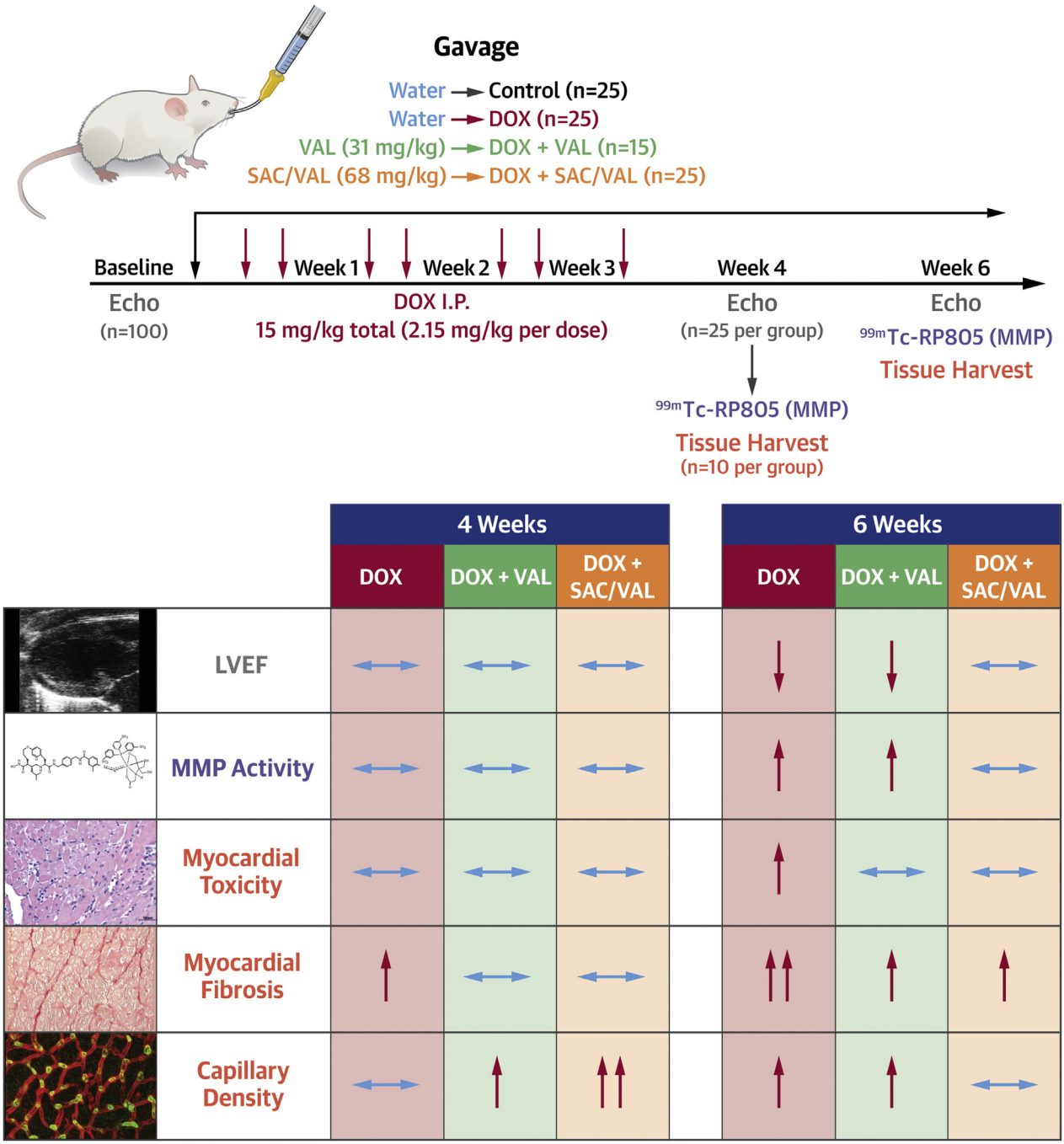

Boutagy, N.E. et al. J Am Coll Cardiol CardioOnc. 2020;2(5):774–87.

Continued on the next page

lines, a recent study showed that Sac/Val was able to attenuate dilated cardiomyopathy and cellular evidence of toxicity in mice administered high-dose DOX (21). Although providing the first report of the efficacy of Sac/Val as a cardioprotective agent against AIC, the lack of a comparator group did not allow for determination of potential advantage of Sac/Val compared with standard RAAS inhibition therapy. Furthermore, the high dosing regimen produced rapid dilated cardiomyopathy that does not recapitulate clinically

TABLE 1 Description of Pathological Scorning System

Category	Description of Pathology	Score
Myofiber vacuolation, and/or myofiber atrophy or degeneration	Cluster of myofibers with typical intracytoplasmic vacuolations and/or regions of myofiber atrophy, disorganization, or degeneration	0 = normal histological appearance 1 = <10%/section 2 = 10%–20%/section 3 = >20%/section
Increased cellularity, associated with myofiber degeneration or vacuolation	Inflammation (macrophages, lymphocytes) or fibroplasia associated with evidence of myofiber injury	

observed AIC, which is progressive and typically is detected after completion of chemotherapy (27). Our study extends these findings, as we show that Sac/Val was able preserve LV systolic function and reduce histological evidence of cardiac injury and fibrosis in an established rodent model of progressive AIC, whereas Val was only able to reduce histological evidence of cardiac injury in this model.

Accumulating evidence in both small and large animals implicate alterations in myocardial MMP activity as a mediator in anthracycline-induced cardiac remodeling and subsequent contractile dysfunction (9,28). However, the temporal pattern of MMP activation appears to be dependent on the dosing regimen. Specifically, acute studies employing a single high dose of DOX observe early increases in MMP-2 (28), whereas delayed myocardial MMP expression (MMP-2 and MMP-9) and activation patterns were detected with chronic low-dose administration protocols (3,9). Despite these temporal differences, these observations confirm that MMP activation is associated with overt cardiac remodeling and dysfunction in these models, thus suggesting acute and sustained myocardial MMP activation as a key cellular event in the initiation and progression of AIC. In this current study, we demonstrate for the first time using ^{99m}Tc-RP805, a sensitive index of myocardial MMP activity, that Sac/Val was able to significantly attenuate myocardial MMP activation in DOX-treated rats. In addition, despite the attenuation of myocellular toxicity and fibrosis, treatment of DOX rats with Val did not significantly influence myocardial ^{99m}Tc-RP805 uptake. These results indicate that the additional beneficial effects afforded by Sac/Val over Val alone in this model of AIC are due in part to a reduction in myocardial MMP activity. In line with these findings, a recent study in rats showed that Sac/Val therapy following coronary ligation attenuated cardiac rupture compared with enalapril, and this was partially attributed to a significant reduction in MMP-9 activation in the infarct region of the myocardium (29). Although tempting to speculate parallels between our studies, studies are needed to fully elucidate the cellular and molecular underpinnings of our findings.

Natriuretic peptides have been shown to have direct antifibrotic, antihypertrophic, and proangiogenic effects (30). Therefore, we assessed some of these parameters with immunohistochemistry to shed some light on our observations of greater cardioprotection afforded by Sac/Val over Val alone. Both Val and Sac/Val treatment afforded some protection against DOX-induced fibrosis, whereas neither treatment was able to prevent DOX-induced myocardial atrophy. Interestingly, we observed an early, robust increase in capillary density in Sac/Val-treated rats compared with DOX-alone animals. DOX rats treated with Val also demonstrated an early increase in capillary density, albeit to a lesser magnitude compared with Sac/Val-treated rats. At the terminal time point, both DOX-alone and DOX + Val rats displayed an elevation in capillary density compared with control animals, whereas capillary

CENTRAL ILLUSTRATION Continued

Echocardiography was performed at baseline in all rats (n = 100). Rats were then administered doxorubicin (DOX) (2.15 mg/kg) every 3 days for 21 days (15 mg/kg total) (n = 75) or an equal volume of 0.9% saline (control animals, n = 25) intraperitoneally. After the first dose, DOX rats remained untreated (DOX, n = 25), or were administered valsartan (Val) (31 mg/kg; DOX+ Val, n = 25) or sacubitril (Sac)/Val (68 mg/kg; DOX+ Sac/Val, n = 25) by gavage for the duration of study. Control and DOX-alone animals were gavaged with water. At 4 weeks post-chemotherapy, echocardiography-derived left ventricular (LV) function (LV ejection fraction), in vivo myocardial matrix metalloproteinase activity (following ^{99m}Tc-RP805 injection) or histological myocardial toxicity as assessed by hematoxylin and eosin and Masson's Trichrome staining was no different **(blue horizontal double-sided arrow)** in the DOX groups compared with control animals. At this time point, myocardial fibrosis (Picrosirius red) was only increased **(red arrow)** in the DOX-alone group but was prevented with Val and Sac/Val treatment compared with time-matched control animals. Note that, α-smooth muscle actin levels—an index of early fibrosis—were elevated in all DOX-treated animals regardless of treatment at this time (not shown). At this early time point, capillary density was increased in rats treated with DOX with either Val or Sac/Val compared with control animals, with a greater increase observed in the Sac/Val group. At 6 weeks post-chemotherapy, LV ejection fraction was decreased in the DOX and in DOX + Val animals compared with time-matched control animals but was preserved with DOX + Sac/Val therapy. Matrix metalloproteinase activation was increased in the myocardium of DOX and in DOX + Val rats compared with time-matched control animals but was not different in DOX + Sac/Val rats. Myocardial toxicity increased in the DOX group at this later time point compared with control animals but was prevented by both Val and Sac/Val treatment. At 6 weeks, myocardial fibrosis was increased in the DOX-alone rats compared with control animals. In addition, myocardial fibrosis was increased in both the Val and Sac/Val groups relative to control animals, albeit this increase was less than that observed in DOX-alone rats at this time point. Last, capillary density was higher in DOX and DOX + Val rats compared with control animals at this later time point, whereas it was no different from control animals in the Sac/Val-treated rats.

density in Sac/Val rats was similar to control animals at this later time point. These findings suggest a rapid and potentially beneficial response in Sac/Val rats that may have contributed to preserved myocardial function in these animals. The temporal patterns of an early, robust increase in capillary density, followed by a subsequent return to basal levels is in line with angiogenesis patterns following acute injury. Specifically, our group recently showed Sac/Val therapy stimulates an early increase in ^{99m}Tc-NC100692 (a radiotracer that binds to proliferating endothelial cells) in the infarct region of rats following permanent left anterior descending artery ligation. Similar to the AIC model, ^{99m}Tc-NC100692 returns to control levels at later time points post-infarct (19). Interestingly, studies in mice have demonstrated that stimulating angiogenesis with vascular endothelial growth factor B gene therapy attenuates myocardial injury associated with acute and chronic DOX administration (31). However, it is worth noting that capillary density is often reduced with DOX administration in murine models (31,32), rather than increased as observed in this model. The reason for this discrepancy is unknown, but species, dosing regimen, and length of follow-up may contribute to these differences. Indeed, more detailed molecular analyses are needed to confirm our observations, as well as uncover other mechanisms that may be contributing to the greater cardioprotective actions afforded by Sac/Val over Val alone.

STUDY LIMITATIONS. First, we did not measure circulating natriuretic peptides or renal neprilysin activity in this study. Thus, despite offering greater protection against LV remodeling and dysfunction compared with standard ARB therapy, we do not know the magnitude of neprilysin inhibition afforded by the Sac/Val dosing regimen used in our study. However, it is worth mentioning that previous preclinical studies demonstrated adequate neprilysin inhibition in rats using a similar dosing scheme of Sac/Val as used in this study (22). Second, we were unable to accurately quantify diastolic function in these animals due to mitral valve E- and A-wave fusion. Thus, we cannot exclude the possibility of diastolic dysfunction in our model and the potential benefit of Val or Sac/Val on these parameters. Third, our use of intraperitoneal injections of DOX, in an effort to prevent extravasation, led to ascites secondary to liver damage. Thus, the length of follow-up and the ability to perform invasive hemodynamic measurements were limited at later time points in these animals. Therefore, we cannot determine whether protection afforded by Sac/Val would have been more evident with more severe cardiotoxicity, nor can we rule out that the Sac/Val effects on LV remodeling and dysfunction were in part due to alterations in preload or afterload. Therefore, to fully realize the full potential of Sac/Val in the setting of chronic DOX administration, future studies should employ large animal models, in which intravenous injection of DOX and arterial pressures are more easily applied, as recently described by our group (33). Lastly, healthy rats were used in this study; thus, whether Sac/Val therapy interferes with the antineoplastic effects of DOX is unknown at this juncture. Thus, future studies evaluating Sac/Val in the setting of AIC should employ tumor-bearing models to rule out this possibility.

CONCLUSIONS

Sac/Val resulted in greater benefit than Val therapy in protecting against LV remodeling and dysfunction in a progressive rodent model of AIC. Importantly, the preservation of LVEF with Sac/Val therapy in DOX rats was associated with only mild myocardial toxicity and no significant changes in MMP activity. On the other hand, Val therapy alone only attenuated DOX-induced toxicity and fibrosis at the cellular level but failed to preserve LVEF and inhibit myocardial MMP activation. Thus, these data suggest that the preservation of LVEF with Sac/Val is due in part to a reduction in myocardial MMP activity. Future investigations should focus on evaluating the ability of Sac/Val to inhibit MMP activation and preserve cardiac function in the setting of chemotherapy-induced cardiotoxicity in large animal models and in cancer patients (NCT03760588).

ACKNOWLEDGMENTS We gratefully acknowledge the technical staff of Yale Translational Research Imaging Center, especially Daniela Orozco, MS; Tsa Shelton, MS; and Christi Hawley.

AUTHOR DISCLOSURES

This study was supported National Institutes of Health grant nos. T32HL098069 (to Dr. Sinusas), S10RR023602 (to Dr. Young), and Novartis Pharmaceuticals grant no. LCZ696BUSNC17T (to Drs. Sinusas and Boutagy). Drs. Spinale and Sinusas are founders of MicroVide, LLC, which holds the license for the use of ^{99m}Tc-RP805 in myocardial applications. All other authors have reported that they have no relationships relevant to the contents of this paper to disclose.

ADDRESS FOR CORRESPONDENCE: Dr. Albert J. Sinusas, Section of Cardiovascular Medicine, Yale University School of Medicine, P.O. Box 208017, Dana 3, New Haven, Connecticut 06520-8017, USA. E-mail: albert.sinusas@yale.edu. Twitter: @nabilboutagy, @attilafehermd, @YTRIC1.

PERSPECTIVES

COMPETENCY IN MEDICAL KNOWLEDGE: This study provides the first evidence that Sac/Val, a first-in-class angiotensin receptor-neprilysin inhibitor, resulted in greater preservation of cardiac systolic function and remodeling than standard ARB with valsartan in an established rodent model of progressive AIC. Both Val and Sac/Val attenuated histological evidence of myocardial degeneration and fibrosis, but only Sac/Val therapy attenuated late elevations in myocardial proteolytic enzyme activity (MMPs). Together, these findings suggest that the preservation of systolic function with Sac/Val is due, at least in part, to altered extracellular matrix remodeling secondary to a reduction in myocardial MMP activity.

TRANSLATIONAL OUTLOOK: Studies in large animal models of AIC and in cancer patients receiving anthracycline chemotherapy (e.g., NCT03760588) are warranted to determine the potential clinical efficacy of Sac/Val as a therapy to treat cardiotoxicity. As circulating MMPs and TIMPs have been used as early indices of cardiotoxicity, future clinical studies may include both quantitative imaging (molecular and functional) and circulating biomarkers as therapeutic endpoints.

REFERENCES

1. Yeh ET, Bickford CL. Cardiovascular complications of cancer therapy: incidence, pathogenesis, diagnosis, and management. J Am Coll Cardiol 2009;53:2231–47.

2. Cardinale D, Colombo A, Lamantia G, et al. Anthracycline-induced cardiomyopathy clinical relevance and response to pharmacologic therapy. J Am Coll Cardiol 2010;55:213–20.

3. Boutagy NE, Wu J, Cai Z, et al. In vivo reactive oxygen species detection with a novel positron emission tomography tracer, 18F-DHMT, allows for early detection of anthracycline-induced cardiotoxicity in rodents. J Am Coll Cardiol Basic Trans Science 2018;3:378–90.

4. Chan BY, Roczkowsky A, Cho WJ, et al. MMP inhibitors attenuate doxorubicin cardiotoxicity by preventing intracellular and extracellular matrix remodeling. Cardiovasc Res 2020 Jan 29 [E-pub ahead of print].

5. Su H, Spinale FG, Dobrucki LW, et al. Noninvasive targeted imaging of matrix metalloproteinase activation in a murine model of postinfarction remodeling. Circulation 2005;112:3157–67.

6. Xue C-B, Voss ME, Nelson DJ, et al. Design, synthesis, and structure– activity relationships of macrocyclic hydroxamic acids that inhibit tumor necrosis factor α release in vitro and in vivo. J Med Chem 2001;44:2636–60.

7. Sahul ZH, Mukherjee R, Song J, et al. Targeted imaging of the spatial and temporal variation of matrix metalloproteinase activity in a porcine model of postinfarct remodeling: relationship to myocardial dysfunction. Circ Cardiovasc Imaging 2011;4:381–91.

8. Goetzenich A, Hatam N, Zernecke A, et al. Alteration of matrix metalloproteinases in selective left ventricular adriamycin-induced cardiomyopathy in the pig. J Heart Lung Transplant 2009;28:1087–93.

9. Ivanová M, Dovinová I, Okruhlicová Ľ, et al. Chronic cardiotoxicity of doxorubicin involves activation of myocardial and circulating matrix metalloproteinases in rats. Acta Pharmacol Sin 2012;33:459–69.

10. Toro-Salazar OH, Lee JH, Zellars KN, et al. Use of integrated imaging and serum biomarker profiles to identify subclinical dysfunction in pediatric cancer patients treated with anthracyclines. Cardiooncology 2018;4:4.

11. Toko H, Oka T, Zou Y, et al. Angiotensin II type 1a receptor mediates doxorubicin-induced cardiomyopathy. Hyperten Res 2002;25:597–603.

12. Akolkar G, Bhullar N, Bews H, et al. The role of renin angiotensin system antagonists in the prevention of doxorubicin and trastuzumab induced cardiotoxicity. Cardiovasc Ultrasound 2015;13:18.

13. Zong WN, Yang XH, Chen XM, et al. Regulation of angiotensin-(1–7) and angiotensin II type 1 receptor by telmisartan and losartan in adriamycin-induced rat heart failure. Acta Pharmacol Sin 2011;32:1345–50.

14. Cadeddu C, Piras A, Mantovani G, et al. Protective effects of the angiotensin II receptor blocker telmisartan on epirubicin-induced inflammation, oxidative stress, and early ventricular impairment. Am Heart J 2010;160:487.e1–7.

15. Cardinale D, Colombo A, Sandri MT, et al. Prevention of high-dose chemotherapy-induced cardiotoxicity in high-risk patients by angiotensin-converting enzyme inhibition. Circulation 2006;114:2474–81.

16. Spallarossa P, Guerrini M, Arboscello E, Sicbaldi V. Enalapril and carvedilol for preventing chemotherapy-induced left ventricular systolic dysfunction. J Am Coll Cardiol 2013;62:2451–2.

17. Georgakopoulos P, Roussou P, Matsakas E, et al. Cardioprotective effect of metoprolol and enalapril in doxorubicin-treated lymphoma patients: a prospective, parallel-group, randomized, controlled study with 36-month follow-up. Am J Hematol 2010;85:894–6.

18. McMurray JJ, Packer M, Desai AS, et al. Angiotensin-neprilysin inhibition versus enalapril in heart failure. N Engl J Med 2014;371:993–1004.

19. Pfau D, Thorn SL, Zhang J, et al. Angiotensin receptor neprilysin inhibitor attenuates myocardial remodeling and improves infarct perfusion in experimental heart failure. Sci Rep 2019;9:5791.

20. Kompa AR, Lu J, Weller TJ, et al. Angiotensin receptor neprilysin inhibition provides superior cardioprotection compared with angiotensin converting enzyme inhibition after experimental myocardial infarction. Int J Cardiol 2018;258:192–8.

21. Xia Y, Chen Z, Chen A, et al. LCZ696 improves cardiac function via alleviating Drp1-mediated mitochondrial dysfunction in mice with doxorubicin-induced dilated cardiomyopathy. J Mol Cell Cardiol 2017;108:138–48.

22. Gu J, Noe A, Chandra P, et al. Pharmacokinetics and pharmacodynamics of LCZ696, a novel dual-acting angiotensin receptor–neprilysin inhibitor (ARNi). J Clin Pharmacol 2010;50:401–14.

23. Dazzi H, Kaufmann K, Follath F. Anthracycline-induced acute cardiotoxicity in adults treated for leukaemia: Analysis of the clinico-pathological aspects of documented acute anthracycline-induced cardiotoxicity in patients treated for acute leukaemia at the University Hospital of Zürich, Switzerland, bet ween 1990 and 1996. Ann Oncol 2001;12:963–6.

24. Rochette L, Guenancia C, Gudjoncik A, et al. Anthracyclines/trastuzumab: new aspects of cardiotoxicity and molecular mechanisms. Trends Pharmacol Sci 2015;36:326–48.

25. Arozal W, Watanabe K, Veeraveedu PT, et al. Effect of telmisartan in limiting the cardiotoxic

effect of daunorubicin in rats. J Pharm Pharmacol 2010;62:1776–83.

26. Silber JH, Cnaan A, Clark BJ, et al. Enalapril to prevent cardiac function decline in long-term survivors of pediatric cancer exposed to anthracyclines. J Clin Oncol 2004; 22:820–8.

27. Russell RR, Alexander J, Jain D, et al. The role and clinical effectiveness of multimodality imaging in the management of cardiac complications of cancer and cancer therapy. J Nucl Cardiol 2016;23: 856–84.

28. Polegato BF, Minicucci MF, Azevedo PS, et al. Acute doxorubicin-induced cardiotoxicity is associated with matrix metalloproteinase-2 alterations in rats. Cell Physiol Biochem 2015;35: 1924–33.

29. Ishii M, Kaikita K, Sato K, et al. Cardioprotective effects of LCZ696 (sacubitril/valsartan) after experimental acute myocardial infarction. J Am Coll Cardiol Basic Trans Science 2017;2:655–68.

30. Nishikimi T, Maeda N, Matsuoka H. The role of natriuretic peptides in cardioprotection. Cardiovasc Res 2006;69:318–28.

31. Räsänen M, Degerman J, Nissinen TA, et al. VEGF-B gene therapy inhibits doxorubicin-induced cardiotoxicity by endothelial protection. Proc Natl Acad Sci U S A 2016;113:13144–9.

32. Coppola C, Riccio G, Barbieri A, et al. Antineoplastic-related cardiotoxicity, morphofunctional aspects in a murine model: contribution of the new tool 2D-speckle tracking. Onco Targets Ther 2016;9:6785–94.

33. Feher A, Boutagy NE, Stendahl JC, et al. Computed tomographic angiography assessment of epicardial coronary vasoreactivity for early detection of doxorubicin-induced cardiotoxicity. J Am Coll Cardiol CardioOnc 2020; 2:207–19.

KEY WORDS anthracycline, echocardiography, preclinical study, treatment

APPENDIX For expanded Methods and Reference sections as well as a supplemental figure and table, please see the online version of this paper.